cause of the critical dependence of turbulence start-stop points on subjective editing procedures.

An important consideration for future commerical aviation flights in the stratosphere is the impact of meteorological conditions, such as the Australian winter jet, on route structure. Will the threat of moderate or severe turbulence result in costly rerouting around areas prone to strong winds? It is possible that commercial aviation routes in use today at lower altitudes will not be acceptable for supersonic flights in the stratosphere if low frequency, large amplitude turbulence is prevalent over certain regions. Some of the apparent difficulties facing the supersonic aircraft may be better understood with further analysis of the HICAT data. Flight data tapes are available for all turbulence encounters, along with oscillograph records of each flight. Future tasks could include analysis of the variance of the first and second most important parameters controlling the distribution of turbulence.

References

[1]Ashburn, E. V. and Waco, D. E., "Ratio of Turbulent Flight Miles to Total Flight Miles in the Altitude Range 45,000–65,000 Ft," *Journal of Aircraft*, Vol. 8, No. 2, Feb. 1971, pp. 127–128.

[2]Ashburn, E. V., "Distribution of Lengths of High Altitude Clear Air Turbulence Regions," *Journal of Aircraft*, Vol. 6, No. 4, Jul.-Aug. 1969, pp. 381–382.

Model Tests on Unsteady Rotor Wake Effects

Kurt H. Hohenemser* and S. T. Crews†
Washington University, St. Louis, Mo.

Nomenclature

t = nondimensional time
β = blade flapping angle, positive up
θ = blade pitch angle, positive nose up
β_I,β_{II} = forward and left rotor tilting angle
θ_I,θ_{II} = forward and left cyclic pitch angle
θ_o = collective pitch angle
μ = rotor advance ratio
ω = nondimensional frequency of progression or regression in airframe fixed reference system

Introduction

STEADY-STATE wake asymmetrics have been shown to result in large reductions in hingeless rotor cyclic control effectiveness[1] and in substantial changes of hingeless rotor static derivatives not only at low but also at high advance ratios.[2] Unsteady substall rotor aerodynamics, recently summarized by Pierce and White[3] are usually based on the rigid vortex wake concept, where the spacing of the wake vortices is preselected independent of blade motions. This concept appears to be ill-suited for the conditions of the model tests to be reported on here, where low frequency progressing or regressing flapping modes are excited at low lift. Related rotor model tests and supporting analysis reported by Kuczynski, Sharpe and Sissingh[4] used single-axis harmonic excitation of the cyclic controls. Unsteady wake effects may have been present but were not identified, possibly because of compensating influences of the neglected blade flexibility and the neglected wake in the analysis. Test results to be presented in the following were obtained with progressing and regressing cyclic control excitation. One reason for selecting this form of excitation was the desire for simplicity of the rotor model which did not require actuators nor a swashplate nor control links with their unavoidable play, but which used instead actuation of the feathering motion by an excentric. Another more basic reason was that dynamic instabilities caused by interblade coupling occur in the form of advancing or regressing blade flapping[5] so that it is of particular interest to find out what unsteady wake interactions exist for such modes.

A Qualitative Model of Unsteady Asymmetric Wake Effects

We first consider a progressing blade flapping mode in which each blade flaps in a rotating frame of reference with the non-dimensional period $2\pi/(1-\omega)$ which is longer than the period of rotation 2π and which is also longer than the natural blade flapping period. The sum of elastic, centrifugal and inertia flapping moments about the rotor center is directed opposite to the flapping deflection β. To sustain an advancing flapping mode the aerodynamic flapping moment on each blade at the phase of maximum up β must be directed upward, causing a dynamic downwash. The opposite blade will have at the same time its maximum down β and will cause an upwash. We thus have a progressing asymmetrical wake. Because of wake inertia the wake will lag the blade oscillation. Thus each blade when passing the neutral position on its way up, will encounter a downwash which is equivalent to an increased aerodynamic damping. In a regressing blade flapping mode the wake will lead the blade flapping oscillation in a rotating frame of reference. We have now two cases. Either the blade operates below resonance, then we have downwash at the phase of maximum up blade flapping, and, because of the lead of the wake, a decreased aerodynamic damping. Or the blade operates above resonance, then we have upwash at the phase of maximum up blade flapping and because of the lead of the wake increased aerodynamic damping. When the blade is in resonance and has zero mechanical damping, no aerodynamic moment is required to sustain the flapping oscillation and no wake occurs. Since in most rotor designs, the blade resonance frequency is only slightly above the rotational frequency, the unsteady wake effect will mostly increase blade aerodynamic damping and will thereby decrease the airframe damping which is important for whirl flutter, air resonance and flying qualities.

Test Equipment and Calibration

The rotor model used for the tests is two bladed with 16 in. diam and 1-in. blade chord. The airfoil is NACA 0012. The blades are attached to the hub with soft flexures, giving first flap bending frequencies of 11.6 and 24.3 *cps* at 0 and 20.3 *rps* rotor speed, respectively. Second flap bending frequency, first torsional frequency and first chordwise frequency at 20.3 *rps* are 161, 184, and 200 *cps*, respectively. The blade Lock number is 4.0. Fig. 1 shows a schematic of hub and pitch control with blade flexure F, feathering shaft S oscillated by a bending spring B from an excentric E, driven by an internal shaft I. A feathering amplitude of ±1.5° was used for the tests. The internal shaft I is driven by a set of exchangeable gears from the rotor shaft and can rotate with 0, ±0.05, ±0.1, ±0.2, ±0.6, ±0.8 times rotor speed. Both shafts carry magnetic pickups to measure the azimuth angles and shaft speeds. One blade flexure is strain gauged for blade flap bending, the other

Received October 2, 1972; revision received October 30, 1972. Sponsored by the Ames Directorate, AAMRDL under Contract NAS2-4151.

Index category: VTOL, Rotary Wing Aerodynamics.

*Professor, Department of Mechanical & Aerospace Engineering. Associate Fellow AIAA.

†Graduate Research Assistant, Department of Mechanical & Aerospace Engineering.

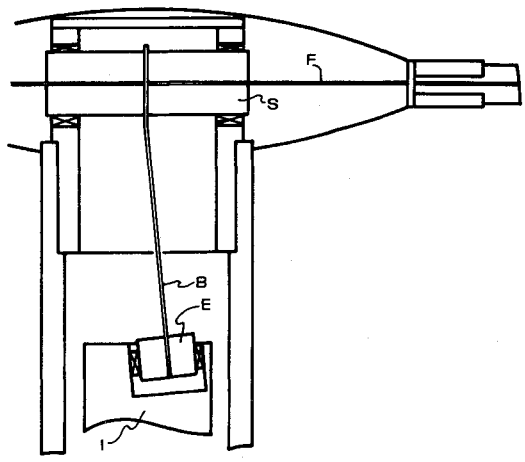

Fig. 1 Schematic of hub and pitch control.

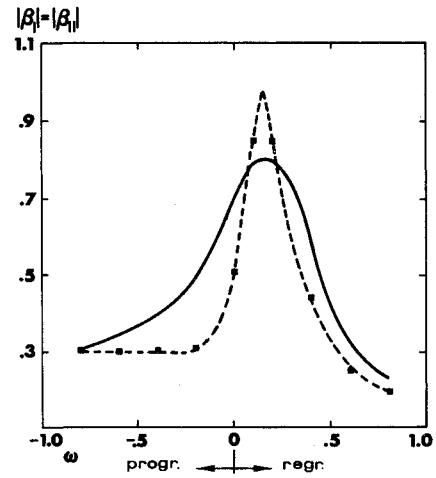

Fig. 2 Rotor tilting amplitude per unit cyclic pitch amplitude, $\mu = 0$, $\theta_0 = 5°$.

for blade torsion. The rotor shaft and hub are faired so that the installation is aerodynamically very clean. Since the entire control system has only 3 high precision bearings, see Fig. 1, the play in the controls in practically zero, while conventional rotor models have unavoidable large play.

The open return wind tunnel has a 24 × 24 in. test section. The flow is remarkably uniform. To avoid flow breakdown at low tunnel speed, the lowest rotor advance ratio tested was 0.2. Conditions of zero advance ratio were tested outside the wind tunnel. When the rotor shaft is turning and the excentric shaft is fixed, steady cyclic pitch is applied. Progressing or regressing flapping modes are excited by turning the inner shaft in the direction or opposite the direction of rotor rotation.

The blade natural frequencies at zero rotor speed were determined very accurately by exciting the blade with a magnetic exciter and by determining electronically the frequency for 90° phase shift between response and excitation. Frequency, mode shapes and flap bending moments, nonrotating and rotating, were determined by a finite element analysis with 20 elements of unequal length, using a smaller length in the region of the flexure, where the curvature is large. Blade mass and bending stiffness are uniform except for the region of the flexure. The bending stiffness was adjusted in the analysis until complete agreement between test and analysis for both first and second blade natural bending frequencies was achieved. For analysis and experiment the flapping angle β is arbitrarily defined by the straight line from the rotor center to the first mode deflection at 0.66 radius. The flap-bending moment per degree flapping at the strain gauge location at 20.3 rotor rps is 0.062 in lb/deg, a value which was determined both analytically and experimentally by deflecting the blade under simulated centrifugal force.

Data Processing and Results

The analytical flapping response with which the experimental response is compared, was obtained from a linear analysis which included flap bending flexibility in the first mode, but which excluded wake effects.‡ The tests were conducted within the linear lift range. The rotor was found in hovering to begin stalling at 11° collective pitch setting, corresponding to a blade angle of attack at 0.7 radius of about 7°.

The separation of the rotor tilting response from the rotor warping response and from the trim effects is performed in the following way. The equations are written for the progressing mode. For the regressing mode the sign for ω must be reversed. The cyclic pitch excitation in the rotating frame of reference is

$$\theta = |\theta| \exp it(1-\omega) = (\cos t + i \sin t) \exp(-it\omega) \quad (1)$$

The flapping response is of the form

$$\beta = [F_1(t) + iF_2(t)] \exp(-i\omega t) + \ldots \quad (2)$$

The symbol + . . . stands for the harmonics with frequency 1, 2, . . . from the trim response. We write

$$\left.\begin{aligned} F_1(t) &= F_{1c} \cos t + F_{1s} \sin t + \ldots \\ F_2(t) &= F_{2c} \cos t + F_{2s} \sin t + \ldots \end{aligned}\right\} \quad (3)$$

where the symbol + . . . now stands for the harmonics with frequency 2, 3, . . . from the rotor plane warping response, while the first harmonics define rotor tilting. Inserting Eq. (3) in Eq. (2) and taking real parts, input and response are

$$\theta = |\theta| \cos(1-\omega)t \quad (4)$$

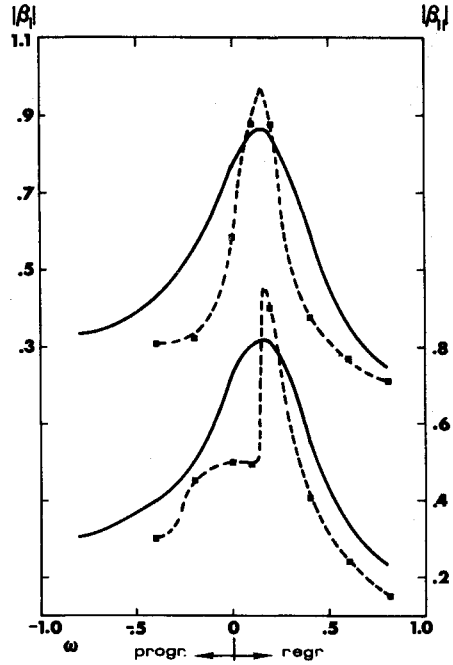

Fig. 3 Rotor tilting amplitude per unit cyclic pitch amplitude, $\mu = 0.2$, $\theta_0 = 5°$.

‡The analysis was performed by S. K. Yin.

$$\begin{aligned}\beta &= F_{1c}\cos t\cos\omega t + F_{1s}\sin t\cos\omega t \\ &+ F_{2c}\cos t\sin\omega t + F_{2s}\sin t\sin\omega t + \ldots \\ &= A_{1c}\cos(1+\omega)t + A_{1s}\sin(1+\omega)t \\ &+ A_{2c}\cos(1-\omega)t + A_{2s}\sin(1-\omega)t + \ldots\end{aligned} \tag{5}$$

Equating the coefficients of the 4 harmonics we have

$$\begin{aligned}F_{1c} &= A_{1c} + A_{2c}, \quad F_{1s} = A_{1s} + A_{2s} \\ F_{2c} &= A_{1s} - A_{2s}, \quad F_{2s} = A_{2c} - A_{1c}\end{aligned} \tag{6}$$

In order to obtain the tilting response in the form of Eqs. (2) and (3) we merely have to determine from the measured flapping response $\beta(t)$ the 4 Fourier coefficients for the harmonics $1+\omega$ and $1-\omega$ and then use Eq. (6). The base frequency for the Fourier analysis of the response $\beta(t)$ must be selected such that both $1+\omega$ and $1-\omega$ are integer multiples of this base frequency.

In an air frame fixed reference system and using again complex notation we have from Eq. (1) the cyclic pitch excitation

$$\left.\begin{aligned}\theta_I &= -i|\theta|\exp(-i\omega t) \text{ forward} \\ \theta_{II} &= |\theta|\exp(-i\omega t) \quad \text{left}\end{aligned}\right\} \text{ control} \tag{7}$$

and from Eqs. (2) and (3) the tilting response

$$\left.\begin{aligned}\beta_I &= (F_{1c} + iF_{2c})\exp(-i\omega t) \text{ forward} \\ \beta_{II} &= (F_{1s} + iF_{2s})\exp(-i\omega t) \text{ left}\end{aligned}\right\} \text{ tilt} \tag{8}$$

For unit cyclic pitch, $|\theta| = 1$, the response amplitudes are

$$\left.\begin{aligned}|\beta_I| &= (F_{1c}^2 + F_{2c}^2)^{1/2} \\ |\beta_{II}| &= (F_{1s}^2 + F_{2s}^2)^{1/2}\end{aligned}\right\} \tag{9}$$

The phase differences between response and input are

$$\left.\begin{aligned}\psi_I &= \text{ang}\beta_I - \text{ang}\theta_I = \text{ang}(F_{1c} + iF_{2c}) + \pi/2 \\ \psi_{II} &= \text{ang}\beta_{II} - \text{ang}\theta_{II} = \text{ang}(F_{1s} + iF_{2s})\end{aligned}\right\} \tag{10}$$

Examples of the measured and computed tilting response amplitudes according to Eq. (9) are shown in Figs. 2 and 3.

The preceding method of separating the cyclic control response from the trim response does not work for $\omega = 0$ so that for steady control inputs the trim response must be measured separately and subtracted from the total response. Data processing according to the preceding equations was performed from the magnetic tape records on a PDP-12 analog-digital converter and computer.

Figs. 2 and 3 show for zero rotor shaft angle, 5° collective pitch setting and advance ratios 0 and 0.2, respectively a comparison of analytical (solid lines) and test (dash lines) amplitudes per unit cyclic pitch input. For $\omega = 0.2$, corresponding to the blade natural frequency, the two curves intersect indicating the absence of a wake effect. At other frequencies large systematic deviations in test response from the analytical response occur, following the trend of the qualitative model explained before. Reference 6 includes more test conditions and also phase angle plots from Eq. (8). The data processing method given in Ref. 6 is somewhat different from that given here. The results are the same.

Conclusions

Progressing and regressing rotor flapping modes can be easily excited with a very simple two-bladed rotor model with only 3 control bearings. The unsteady wake effects are largest at zero advance ratio and low collective pitch, but they remain significant at higher advance ratios and collective pitch settings. A more detailed study of the phenomenon to cover a wider test envelope, ground effects and direct wake measurements is in progress.

References

[1]Miller, R. H., "Rotor Blade Harmonic Air Loading," *AIAA Journal*, Vol. 2, No. 7, July 1964, p. 1260.

[2]Ormiston, R. A. and Peters, D. C., "Hingeless Rotor Response with Nonuniform Inflow and Elastic Blade Bending," *Journal of Aircraft*, Vol. 9, No. 10, Oct. 1972, pp. 730–736.

[3]Pierce, G. A. and White, W. F., Jr., "Unsteady Rotor Aerodynamics at Low Inflow and its Effects on Flutter," AIAA Paper 72-959, Palo Alto, Calif., 1972.

[4]Kuczinski, W. A., Sharpe, D. L., and Sissingh, G. J., "Hingeless Rotor Experimental Frequency Response and Dynamic Characteristics with Hub Moment Feedback Controls," 28th Annual National Forum of the American Helicopter Society, Preprint 612, May 1972.

[5]Hohenemser, K. H. and Yin, S. K., "Some Applications of the Method of Multiblade Coordinates," *Journal American Helicopter Society*, Vol. 17, No. 3, July 1972, pp. 3–12.

[6]Hohenemser, K. H. and Crews, S. T., "Unsteady Wake Effects on Progressing/Regressing Forced Rotor Flapping Modes," AIAA Paper 72-957, Palo Alto, Calif., 1972.

Conformal Mapping for Potential Flow about Airfoils with Attached Flap

Vernon J. Rossow*
NASA Ames Research Center, Moffett Field, Calif.

Introduction

A SURPRISINGLY large number and wide variety of conformal transformations using complex variables are presented in the literature for changing one shape into another (see Betz,[1] Kober,[2] Nehari[3]). A number of these transformations have been used to map a known two-dimensional flowfield into a desired one. For example, most aerodynamicists are familiar with the method developed by Theodorsen[4] as an extension of the Joukowski and Karman-Trefftz transformations which maps the flow about a circular cylinder into that about a specified airfoil. Recently, the Karman-Trefftz method for one circular cylinder/airfoil has been extended by Williams[5] so that the flow about two nearby circles can be mapped into the flow about two lifting airfoils (or about an airfoil with a detached flap). These exact incompressible potential flow solutions are not only useful in themselves but they also serve as reference or check cases for numerical and approximate methods.

The purpose of this Note is to present a conformal mapping sequence that transforms the potential flow about a circle into that about an airfoil with an attached flap or spoiler. This method is indirect in that the shape of the flap must be iterated upon by varying parameters in the mapping equations until the resulting flap shape approximates the specified one.

Mapping Sequence

The transformation developed for generating the flap on the airfoil is illustrated in Fig. 1 as 10 steps from a circle

Received September 28, 1972.
Index categories: Airplane and Component Aerodynamics; VTOL Aircraft Design.

* Staff Scientist.